
Schreier-Coset Graph Propagation

Aryan Mishra

Maryland Applied Graduate Engineering
University of Maryland, College Park
amishr17@umd.edu

Lizhen Lin

Department of Mathematics
University of Maryland, College Park
lizhen01@umd.edu

Abstract

Graph Neural Networks (GNNs) offer a principled framework for learning over graph-structured data, yet their expressive capacity is often hindered by over-squashing, wherein information from distant nodes is compressed into fixed-size vectors. Existing solutions, including graph rewiring and bottleneck-resistant architectures such as Cayley and expander graphs, avoid this problem but introduce scalability bottlenecks. In particular, the Cayley graphs constructed over $SL(2, \mathbb{Z}_n)$ exhibit strong theoretical properties, yet suffer from cubic node growth $O(n^3)$, leading to high memory usage. To address this, this work introduces Schreier-Coset Graph Propagation (SCGP), a group-theoretic augmentation method that enriches node features through Schreier-coset embeddings without altering the input graph topology. SCGP embeds bottleneck-free connectivity patterns into a compact feature space, improving long-range message passing while maintaining computational efficiency. Empirical evaluations across standard node and graph classification benchmarks demonstrate that SCGP achieves performance comparable to, or exceeding, expander graph and rewired GNN baselines. Furthermore, SCGP exhibits particular advantages in processing hierarchical and modular graph structures, offering reduced inference latency, improved scalability, and a low memory footprint, making it suitable for real-time and resource-constrained applications.

1 Introduction

Graph Neural Networks (GNNs) are neural network architectures designed to process data exhibiting an inherent graph structure [16]. Their versatility has led to widespread adoption and empirical success across diverse domains and numerous graph-related tasks [36, 1]. Several GNN variants have emerged. For instance, the Graph Convolutional Network (GCN) [21] employs a localized, first-order approximation of spectral graph convolutions. This method aggregates normalized features from neighboring nodes to update node embeddings, achieving a computational complexity that scales linearly with the number of edges, denoted as $O(|E|)$. Another notable architecture is the Graph Isomorphism Network (GIN) [37]. GIN utilizes sum aggregation of neighbor features, followed by a multi-layer perceptron (MLP), to maximize its ability to distinguish between different graph structures. When its MLPs possess sufficient capacity, GIN’s discriminative power is equivalent to the Weisfeiler-Lehman test for graph isomorphism [19]. Most contemporary GNNs operate under the Message Passing Neural Network (MPNN) paradigm [17]. In this framework, nodes iteratively exchange information with their neighbors to refine their representations. While more layers are often necessary to capture long-range interactions within the graph, increasing network depth can lead to challenges. Specifically, the receptive field of nodes grows exponentially with depth. This results in large amounts of information from extensive neighborhoods being compressed into fixed-size embeddings [34]. This phenomenon, known as over-squashing [3], can cause significant information loss [29] and thereby substantially limit the expressive capacity of GNNs [10]. Furthermore, the performance and behavior of GNNs are intrinsically linked to the underlying graph topology. For

example, the Jacobian of node features is influenced by topological properties such as graph curvature and effective resistance [10, 31, 6].

Various methods are employed to address over-squashing in graph neural networks. Graph rewiring techniques by Wilson et al. [34] modify topology using properties like curvature [13, 31], spectral expansion [20, 5], and effective resistance [6] to optimize information flow, though these analyses are computationally intensive. Another approach, Expander Graph Propagation [9], constructs expander graphs, including Cayley graphs [34], to aid propagation. However, Cayley graphs can inflate nodes to $O(n^3)$, requiring memory-intensive padding and truncation, which may disrupt structural properties for instance, 4-regularity, vertex-transitivity, undermine spectral guarantees, and increase computational complexity.

Feature augmentation offers alternative strategies. Laplacian Positional Encoding (LapPE) by Dwivedi et al. [11] injects long-range structural context into node features, reducing the need for deep message-passing layers. However, its $O(n^3)$ eigenvector computation limits scalability and makes it sensitive to topological perturbations. Alternatively, shortest-path distance encoding directly inputs hop counts (all-pair computation is $O(n(|E|))$), bypassing intermediate message propagation. This method typically encodes only scalar distances, thus neglecting information about alternative routes or connectivity issues.

This work introduces **SCHREIER-COSET GRAPH PROPAGATION (SCGP)**, a novel framework leveraging Schreier-coset embeddings from a special linear group to enrich node representations while preserving original graph topology. Distinct from methods that modify the input graph or add connectivity, SCGP enriches node representations via a principled augmentation layer emulating high-expansion graphs’ propagation behavior. This design enables efficient message passing without the overhead of explicit rewiring or superlinear node growth.

The contributions are summarized as follows:

- **Formalization of Schreier-Coset Graphs:** Formalize the generation of Schreier-Coset graphs and describe their incorporation into Graph Neural Networks (GNNs). Their construction involves defining a compact vertex set via group cosets of the special linear group $SL(2, \mathbb{Z}_n)$, selecting suitable generators to form edges, and ensuring deterministic coset representatives. The resulting graphs are bottleneck-resistant and spectrally rich, making them ideal candidates for feature propagation in over-squashed graph neural networks.
- **Theoretical Insights:** Analyze the structural properties of Schreier-Coset graphs utilized by SCGP, highlighting their benefits for message propagation. This research demonstrates that these structural advantages enable SCGP to improve information flow and alleviate over-squashing while maintaining computational efficiency.
- **Empirical Evaluation:** Evaluate the approach through extensive node and graph classification experiments on various widely used benchmark datasets. Numerical results show that SCGP outperforms rewired baselines and Cayley graph-enhanced models, achieving competitive performance with significantly reduced computational burden.

2 Related Work and Existing Approaches

This section reviews prominent techniques designed to alleviate oversquashing in GNNs. A common underlying strategy involves mitigating structural bottlenecks by decoupling the literal input graph (\mathbb{G}) from the computational graph that ultimately governs message-passing dynamics. Alon and Yahav [3] proposed rewiring approaches, such as making the GNN’s final layer fully adjacent. This configuration allows all nodes to interact directly, potentially easing bottlenecks and bypassing the need for extensive full-graph pre-analysis. Graph Transformers [38, 22] further demonstrate this principle by effectively employing full connectivity in every layer. However, such dense approaches impose $O(|V|^2)$ edge complexity typically limits their application to modest graph sizes. Alternatively, Gilmer et al. [15] proposed a ‘controller node’ architecture, introducing a single, central node connected to all other nodes in the graph. While this efficiently reduces the graph’s diameter to 2 with only $O(|V|)$ additional edges, this pivotal controller node can become a new communication bottleneck by over-centralizing information flow.

Graph Rewiring In this approach, the input graph \mathbb{G} is rewired to optimize the spectral or spatial properties of the graph. Karhadkar et al. [20] derived a popular class of approaches based on the

spectral quantity of the graph or by reducing the effective resistance [5, 6, 4]. These approaches have provided compelling insights and reduced over-squashing. However, they impose computational complexity when analyzing the entire input graph structure.

Expander Graph Rewiring The expander graph exhibits the desirable properties associated with spectral gap and effective resistance. Banerjee et al. [5] proposed a construction inspired by expander graphs to rewire the input graph randomly locally, Shirzad et al. [30] uses both virtual nodes and expander graphs as a robust foundation to design the graph transformer architecture. Wilson et al. [34] introduces a combination of virtual nodes and expander graphs for the design of Cayley Propagation, which becomes a bottleneck.

Cayley Graphs Wilson et al. [34] Utilizing GCN and GIN networks, the Cayley graph pipeline, first, inflates the graph to $\Theta(n^3)$ vertices—necessitating extensive padding and straining memory resources. Then, collapse it back to the target input size, a step that fractures the original 4-regular, vertex-transitive structure, undermines its spectral guarantees, and amplifies computational complexity.

Feature Augmentation This method enriches node and edge attributes, appending informative signals, mitigating over-squashing while improving propagation. Eliasof et al. [12] concatenates top- k eigenvectors of the graph Laplacian to every node. Providing each node with global coordination means there is no need for information to travel through many hops. It requires a $O(n^3)$ eigen-decomposition and $O(nk)$ memory, with sign ambiguity and dynamic mini-batches leading it to be less efficient.

3 Schreier-Coset Graph Propagation

3.1 Preliminaries

This section reviews the graph-theoretic and algebraic preliminaries necessary for constructing the Schreier-Coset graph used in the propagation scheme.

An undirected graph is denoted as $\mathbb{G} = (V, E)$ where V is the node and E is the edge. The graph topology is encoded in an adjacency matrix $A \in \mathbb{R}^{|V| \times |V|}$, where A_{ij} denotes the edge between node i and j , and $|V|$ is the number of nodes. Let $D = \text{diag}(\mathbb{G})$ be the diagonal matrix of degrees $D_{vv} = d_v$. The normalized Laplacian $L = \text{lap}(\mathbb{G})$ is defined by $L = D^{-1/2}(D - A)D^{-1/2}$. The eigenvalues of the the normalized Laplacian L are $0 = \lambda_0 \leq \lambda_1 \leq \dots \leq \lambda_{n-2} \leq \lambda_{n-1}$.

Special linear Group $SL(2, \mathbb{Z}_n)$: Let $\mathbb{Z}_n = \mathbb{Z}/n\mathbb{Z}$, denote the ring of integers modulo n . The group $G = SL(2, \mathbb{Z}_n)$ is defined as

$$G = SL(2, \mathbb{Z}_n) = \{M \in \mathbb{Z}_n^{2 \times 2} \mid \det(M) \equiv 1 \pmod{n}\}.$$

n depends on the input graph size. This group serves as the algebraic foundation for constructing both Cayley and Schreier graphs.

Subgroup H : It is considered the subgroup of $H \subset SL(2, \mathbb{Z}_n)$ which consists of diagonal matrices with unit determinant within G :

$$H = \left\{ \begin{pmatrix} a & 0 \\ 0 & d \end{pmatrix} \in G \mid ad \equiv 1 \pmod{n} \right\}.$$

Expander and Cayley Graphs An expander graph has a number of edges that scale linearly with the number of nodes. It is both sparse and highly connected. A family of expander graphs has been precomputed leveraging the theoretical benefits of special linear group $SL(2, \mathbb{Z}_n)$ for which a family of corresponding Cayley Graphs [25] can be derived: $\text{Cay}(SL(2, \mathbb{Z}_n); S_n)$, where S_n denotes a particular generating set for $SL(2, \mathbb{Z}_n)$. For S_n , Cayley graphs have expansion properties and are scalable; however, achieving a large specific number of nodes is not always feasible; the node count for $\text{Cay}SL(2, \mathbb{Z}_n); S_n$ is given by:

$$|V(\text{Cay}((SL(2, \mathbb{Z}_n); S_n)))| = n^3 \prod_{\text{prime } p|n} \left(1 - \frac{1}{p^2}\right),$$

rendering them impractical for large n due to excessive memory requirements. In contrast, Schreier graphs offer a compact alternative by encoding similar group-theoretic structure through cosets, without incurring exponential node growth, the details of which will be provided in the next subsection.

3.2 Schreier-Coset graphs

Schreier-Coset graphs Schreier [26] depict the standard permutation representation of finitely generated group on the cosets of subgroup of $SL(2, \mathbb{Z}_n)$ and provide diagrammatic interpretations of combinational graph theory. The Schreier-Coset graph plays a central role in our propagation scheme, serving as an auxiliary structure that encodes robust expansion and mixing behavior through group-theoretic symmetries. In contrast to traditional augmentation techniques that rewire the input graph directly, our approach constructs a fixed auxiliary graph—independent of the original topology—based on the coset structure of a well-behaved finite group. This section details the construction process of the Schreier-Coset graph \mathcal{S}_n , which is defined over the right coset space of a subgroup H in the group $G = SL(2, \mathbb{Z}_n)$.

Cosets and the Schreier-Coset Graph: The set of right cosets of H in G , denoted by $Hg = \{hg \mid h \in H\}$, forms the *vertex set* \mathcal{V}_S of the Schreier-Coset graph $\mathcal{S}_n = (\mathcal{V}_S, \mathcal{E}_S)$. The *edge set* \mathcal{E}_S is defined via a symmetric generating set $S \subset G$, where each edge represents the group action of a generator on a coset: an edge exists between cosets Hg_1 and Hg_2 if there exists $s \in S$ such that $Hg_2 = Hg_1s$. Since S acts freely on the collections of cosets, each coset corresponds to a distinct class of matrices, and the number of vertices $|\mathcal{V}_S|$ equals the index $|G|/|H|$. Importantly, this yields a significantly smaller vertex set compared to the full Cayley graph over G , enabling more efficient computation.

A typical choice for generators includes elementary row operations:

$$S \approx \left\{ \begin{pmatrix} 1 & \pm 1 \\ 0 & 1 \end{pmatrix}, \begin{pmatrix} 1 & 0 \\ \pm 1 & 1 \end{pmatrix} \right\} \pmod{n}.$$

Canonical Construction: To construct \mathcal{S}_n , it is essential to uniquely identify each coset Hg . Since multiple matrices g can belong to the same coset, a *canonical representation function* $\psi : G \rightarrow \mathcal{V}_S = G/H$ is used. It maps any matrix $M \in Hg$ to a single, unique representative matrix for that coset, ensuring that each distinct coset corresponds to exactly one node during graph construction.

ψ can be defined via lexicographic ordering or other deterministic procedures. The choice of representative does not affect the graph structure, but it simplifies implementation and matrix indexing.

The resulting Schreier-Coset graph \mathcal{S}_n captures structural relationships within $SL(2, \mathbb{Z}_n)$ relative to the subgroup H , induced by the chosen generators S . The Schreier-Coset graph \mathcal{S}_n can be interpreted as a labeled quotient of the Cayley graph $\text{Cay}(G, S)$, where vertices are grouped according to the equivalence relation induced by H . The graph is undirected if S is symmetric, $S = S^{-1}$, which has been assumed throughout.

Structural Properties. Schreier-Coset graphs inherit many favorable properties from the Cayley graphs. They often exhibit strong expansion, spectral gaps, and rapid mixing. While the Cayley graph over $SL(2, \mathbb{Z}_n)$ contains $O(n^3)$ vertices, the Schreier-Coset graph contains significantly fewer, making them more tractable for use in downstream GNN architectures.

Moreover, the graphs are homogeneous because their local structure does not depend on the particular coset, ensuring uniformity in the embeddings learned later. As we will demonstrate, these Schreier graphs are highly expressive despite their compactness and serve as efficient scaffolds for encoding long-range dependencies into node representations.

Example. For instance, consider $n = 5$. The group $SL(2, \mathbb{Z}_5)$ contains 120 elements, while the subgroup H contains 4 diagonal matrices of the form $\left\{ \begin{pmatrix} a & 0 \\ 0 & d \end{pmatrix} \mid ac \equiv 1 \pmod{5}, b \in \mathbb{Z}_5 \right\}$. The first diagonal entry, a , can be any of the 4 elements in \mathbb{Z}_5^\times is 1, 2, 3, 4. d is determined by $d \equiv a^{-1} \pmod{5}$. Now, H contains $|\mathbb{Z}_5^\times| = 4$ matrices. The Schreier-Coset graph \mathcal{S}_5 is constructed with this diagonal subgroup H has $\frac{|G|}{|H|} = \frac{120}{4} = 30$ vertices. The graph generated is smaller and retains important structural properties of the group depicting good connectivity and expansion properties. Figure 1 represents the graphical illustration.

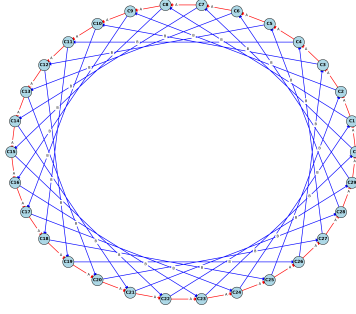


Figure 1: Schreier-Coset graphs constructed is smaller and retains the structural properties of the original graph: connectivity and good expansion characteristics, while being more computationally tractable.

Generating Features from \mathcal{S}_n

The core idea of the augmentation is to distill the structural information from \mathcal{S}_n into fixed-size feature vectors (embeddings) that can be associated with the nodes of the original input graph G_{in} . The generation process proceeds as follows:

1. **Modulus Selection (n):** For an input graph G_{in} with $|V_{in}|$ nodes, an integer $n > 1$ is chosen such that the estimated size of the corresponding Schreier-Coset graph, $|\mathcal{V}_S|$, is greater than or equal to $|V_{in}|$. This ensures the generated structural features have sufficient capacity relative to the input graph size.
2. **Node Count:** The number of nodes in the Schreier-Coset graph is equal to the index of the subgroup H in G . For $G = SL(2, \mathbb{Z}_n)$ and H , the node size is given by :

$$|\mathcal{V}_S| = [SL(2, \mathbb{Z}_n) : H] = \frac{|G|}{|H|}$$

The order of $SL(2, \mathbb{Z}_n)$ is the same as used in the Cayley graph node count. The order of H is $\phi(n)$.

3. **Edge Count :** The number of edges depends on generator S . A symmetric set of 4 generators are used, each node hence has a degree of 4 (though some edges might loop back to the same node or lead to the same neighbor via different generators). Therefore, the total number of directed edges is precisely $|\mathcal{E}_S| = |\mathcal{V}_S| \times |S| = 4 \times |\mathcal{V}_S|$.
4. **Schreier-Coset Graph Generation:** For the selected value of n , the Schreier-Coset graph is constructed as $\mathcal{S}_n = (\mathcal{V}_S, \mathcal{E}_S)$ based canonical coset representation map ψ and the fixed generator set S .
5. **Coset Enumeration Method :** Cosets are enumerated using a Breadth-First Search (BFS) traversal starting from the identity coset H . For each known representative matrix M the neighbors $M' = Ms \pmod{n}$ are computed using generators $s \in S$, a canonicalization function uniquely identifies the resulting set HM' . Edges (HM, HM') for each s are added, and newly identified canonical cosets are queued in BFS for exploration.
6. **Pre-computing Schreier Node Embedding:** The node embeddings are generated as follows:

- Initial features X_S are assigned to nodes in \mathcal{V}_S , commonly taken to be the identity matrix $I_{|\mathcal{V}_S|}$.
- The GCN processes X_S using the Schreier-Coset graph's structure (edges \mathcal{E}_S) for a fixed number of layers. The GCN aggregates neighborhood information within \mathcal{S}_n .

$$H^{(l+1)} = \sigma(\hat{D}^{-1/2} \hat{A} \hat{D}^{-1/2} H^{(l)} W^{(l)}),$$

where \hat{A}, \hat{D} correspond to \mathcal{S}_n , $\sigma(\cdot)$ denotes a nonlinear activation function and $W^{(l)}$ are learned weights.

- Importantly, this process is performed without gradient computation as it's a pre-computation step, not part of the main model training.

- The final output $Z_S \in \mathbb{R}^{|\mathcal{V}_S| \times d_{\text{embed}}}$ from the final GCN layer consists of structural embeddings for the Schreier graph, where $Z_{S,i}$ is the learned embedding for the i -th (node) coset in \mathcal{S}_n .

These precomputed embeddings Z_S form a set of high-level reusable features that capture bottleneck-resistant structural patterns in the Schreier-Coset graph. They are subsequently aligned and injected into the input graph \mathbb{G}_{in} , as described in the following section.

3.3 Integrating Schreier Features into GNN Input

The generated Schreier embeddings Z_S are incorporated into the representation of the feature of the original input graph \mathbb{G}_{in} , creating the input for the main GNN model that will operate on \mathbb{G}_{in} . These structurally informed embeddings serve as an augmentation to the node features of \mathbb{G}_{in} , providing global context derived from the algebraic properties of the auxiliary Schreier-Coset graph \mathcal{S}_n .

1. **Feature Mapping and Resizing:** Since the number of nodes in the Schreier graph, $|\mathcal{V}_S|$, may not equal the number of nodes in the input graph, $|V_{in}|$, the embeddings Z_S need to be mapped or resized. A simple index-based approach is used:

- If $|\mathcal{V}_S| < |V_{in}|$: Z_S is padded with zero vectors to create a matrix of size $|V_{in}| \times d_{\text{embed}}$.
- If $|\mathcal{V}_S| \geq |V_{in}|$: The first $|V_{in}|$ rows of Z_S are selected.

This results in a feature matrix $Z_{S,\text{mapped}} \in \mathbb{R}^{|V_{in}| \times d_{\text{embed}}}$, aligned with the nodes of \mathbb{G}_{in} .

2. **Feature Concatenation:** The mapped Schreier features $Z_{S,\text{mapped}}$ are concatenated with the original node features $X_{in} \in \mathbb{R}^{|V_{in}| \times d_{in}}$ of the input graph along the feature dimension:

$$X_{out} = [X_{in} || Z_{S,\text{mapped}}] \in \mathbb{R}^{|V_{in}| \times (d_{in} + d_{\text{embed}})}$$

3. **Input to Main GNN:** This augmented feature matrix X_{out} replaces the original X_{in} as the initial node feature representation for the input graph \mathbb{G}_{in} . Subsequent layers of the main GNN model will process the graph structure $\mathbb{G}_{in} = (V_{in}, E_{in})$ using these augmented features X_{out} as input.

3.4 Complexity and Practical Considerations

1. **Time Complexity** The generation complexity is polynomial, $O(|\mathcal{V}_S|^{3/2})$, dominated by the $|\mathcal{V}_S|$ cosets and the cost of canonicalization dependent on $\phi(n)$. Although the complexity of Cayley graph generation appears similar per element, its resulting graph is vastly larger. The Schreier-Coset graph's smaller size $O(|\mathcal{V}_S|^{3/2})$ vertices significantly reduces the cost of subsequent processing steps, making it more manageable despite generation overhead.
2. **Memory Caching** In SCGP, caching the computed Schreier-Coset Graph, and the derived embeddings for a given n , is crucial for efficiency while processing multiple input graphs that require the same n avoiding redundant and expensive graph generation, and GNN pre-computation steps.

4 Experiment

In this section, the efficacy of **SCGP** is validated on various node and graph classification datasets and compared with the other state-of-the-art methods. All experiments are conducted on a local server with an NVIDIA A-100 GPU.

4.1 Node Classification

The following datasets have been used for Node Classifications:

Amazon Computers and Amazon Photo [28]: These datasets consist of product co-purchase graphs, where nodes represent items and edges indicate frequent co-purchase relationships. Node features are constructed from bag-of-words representations of product reviews, and class labels correspond to product categories. The Amazon Photo dataset focuses specifically on photographic equipment while preserving identical feature and edge structures.

Table 1: Performance comparison of SCGP against baseline models across six standard benchmark datasets.

Model	Am. Comp.	Am. Photo	CiteS.	Co. CS	Cora	PubMed
LogReg	0.6410 \pm 0.0570	0.7300 \pm 0.0650	-	0.8640 \pm 0.0900	-	-
MLP	0.4490 \pm 0.0580	0.6960 \pm 0.0380	0.5880 \pm 0.0220	0.8830 \pm 0.0070	0.5980 \pm 0.0240	0.7010 \pm 0.0070
GAT	0.7800 \pm 0.1900	0.8570 \pm 0.2030	0.6890 \pm 0.0170	0.9050 \pm 0.0060	0.8080 \pm 0.0160	0.7780 \pm 0.0210
GCN	0.8260 \pm 0.0240	0.9120 \pm 0.0120	0.6820 \pm 0.0160	0.9111 \pm 0.0050	0.7910 \pm 0.0180	0.7880 \pm 0.0060
+ SCGP	0.8884 \pm 0.0269	0.8939 \pm 0.0089	0.6306 \pm 0.0137	0.9119 \pm 0.0095	0.7682 \pm 0.0239	0.7928 \pm 0.0051

CoAuthor CS [28]: A co-authorship network where nodes correspond to authors and edges represent collaborations on at least one publication. Node features are extracted from keywords in the authors’ publications, and classes denote major research areas.

CiteSeer [27]: A citation network where nodes represent scientific articles and edges denote citation relationships. The dataset presents moderate feature sparsity and low average node degree, providing a challenging setting for evaluating message-passing effectiveness.

Cora and PubMed [27]: Benchmark citation networks in which nodes correspond to research papers and edges represent citations. Node features are based on word vector embeddings of paper abstracts, and the classification task involves predicting the subject area.

The evaluation includes two variants: **GCN + SCGP** and **GIN + SCGP**. Each model is trained for 200 epochs using four layers and a dropout rate of 0.5, following the hyperparameter settings from [21]. All experiments are repeated 100 times to ensure statistical robustness. In addition to SCGP-enhanced models, comparisons are made against standard baselines including **LogReg** [8], **MLP** [33], **GAT** [32], and **GCN** [21]. Given that the benchmark datasets exhibit balanced class distributions, test accuracy is adopted as the primary evaluation metric, as reported in **Table 1**.

In **Table 1**, **LogReg** and **MLP** have low performance on most datasets due to their inability to capture the underlying graph structure. In contrast, it effectively integrates structural information, capturing long-range dependencies while maintaining a low memory footprint. It outperforms standard GCNs on the **Amazon Computers** dataset and achieves the highest accuracy on **Coauthor-CS**. Furthermore, SCGP matches or exceeds competitive baselines on four out of six datasets. A slight performance drop is observed on **CiteSeer** and **Cora**, which may be attributed to their planar structure, low graph diameter, and high homophily. Nevertheless, SCGP maintains strong results across diverse graph families, particularly those with modular or hierarchical structure.

4.2 Graph Classification

TU Dataset (see Morris et al. [23]) comprises over 120 graph classification and regression datasets. Representative datasets include chemical graphs (MUTAG), protein structures (PROTEINS), social networks (IMDB-BINARY, REDDIT-BINARY), and research collaboration graphs (COLLAB). The topology of the graphs about the task is identified as requiring long-range interactions. While certain node classification tasks have also been considered in previous works, these are tractable with nearest neighbor information Brockschmidt [7]. **SCGP** is compared against **CGP** Wilson et al. [34], **EGP** Deac et al. [9], **FA** Alon and Milman [2] as well as the following state-of-the-art graph rewiring techniques that require dedicated preprocessing, **DIGL** Gasteiger et al. [14], **SDRF** Topping et al. [31], **FoSR** Karhadkar et al. [20], **BORF** Nguyen et al. [24] and **GTR** Black et al. [6]. The dataset is trained following the Karhadkar et al. [20] experimental setup and hyperparameters for each baseline.

The GNNs are trained with 80% /10 %/10 % , train/val/test split . Leveraging the hyperparameters from Karhadkar et al. [20], the number of layers is fixed to 4 with a hidden dimension of 64 and a dropout of 50%. Accuracy remains the primary metric for the balanced graph structure dataset. OOT indicates out-of-time for the dedicated preprocessing time, and OOM points to out-of-memory error.

SCGP consistently achieves strong performance across diverse datasets within the TU benchmark suite. When applied to GCN and GIN backbones, it attains state-of-the-art accuracy on **TU-ENZYMES**—a dataset that emphasizes long-range dependency modeling - significantly surpassing all baseline methods. SCGP ranks among the top in 5 out of 12 configurations (across six datasets and two architectures), including notable results on **TU REDDIT-BINARY**, **TU COLLAB**, and **TU PROTEINS**, outperforming diffusion-based and geometric models such as **SDRF** [31] and **BORF** [24].

Table 2: Results of SCGP compared against CGP, EGP, FA and the approaches that require dedicated preprocessing for GCN and GIN on the TUDataset. The colors highlight **First**, **Second** and **Third** positions respectively.

Model	REDDIT-BINARY	IMDB-BINARY	MUTAG	ENZYMES	PROTEINS	COLLAB
GCN	77.735 \pm 1.586	60.500 \pm 2.729	74.750 \pm 4.030	29.083 \pm 2.363	66.652 \pm 1.933	70.490 \pm 1.628
+ FA	OOM	48.950 \pm 1.652	70.250 \pm 4.608	28.667 \pm 3.693	71.071 \pm 1.506	72.039 \pm 0.771
+ DIGL	77.350 \pm 1.206	49.600 \pm 2.435	70.500 \pm 5.045	30.833 \pm 1.537	72.723 \pm 1.420	56.470 \pm 0.865
+ SDRF	77.975 \pm 1.479	59.000 \pm 2.254	74.000 \pm 3.462	26.667 \pm 2.000	67.277 \pm 2.170	71.330 \pm 0.807
+ FoSR	77.750 \pm 1.385	59.750 \pm 2.357	75.250 \pm 5.722	24.167 \pm 3.005	70.848 \pm 1.618	67.220 \pm 1.367
+ BORF	OOT	48.900 \pm 0.900	76.750 \pm 0.037	27.833 \pm 0.029	67.411 \pm 0.016	OOT
+ GTR	79.025 \pm 1.248	60.700 \pm 2.079	76.500 \pm 4.189	25.333 \pm 2.931	72.991 \pm 1.956	72.600 \pm 1.025
+ PANDA	87.275 \pm 1.033	68.350 \pm 2.346	76.750 \pm 5.531	30.667 \pm 2.019	70.134 \pm 1.518	73.850 \pm 0.695
+ EGP	67.550 \pm 1.200	59.700 \pm 2.371	70.500 \pm 4.738	27.583 \pm 3.262	73.304 \pm 2.516	69.470 \pm 0.970
+ CGP	67.050 \pm 1.483	56.200 \pm 1.825	83.750 \pm 3.597	31.000 \pm 2.397	73.036 \pm 1.291	69.630 \pm 0.730
+ SCGP	83.860 \pm 0.500	61.400 \pm 1.860	73.950 \pm 3.070	51.920 \pm 3.600	71.350 \pm 1.010	71.580 \pm 0.8100
GIN	84.600 \pm 1.454	71.250 \pm 1.509	80.500 \pm 5.143	35.667 \pm 2.803	70.312 \pm 1.749	71.490 \pm 0.746
+ FA	OOM	69.900 \pm 2.332	80.250 \pm 5.314	47.833 \pm 2.529	72.902 \pm 1.419	72.740 \pm 0.786
+ DIGL	84.575 \pm 1.265	52.650 \pm 2.150	78.500 \pm 4.189	41.500 \pm 3.063	72.321 \pm 1.440	57.620 \pm 1.010
+ SDRF	84.550 \pm 1.396	69.550 \pm 2.381	80.500 \pm 4.177	37.167 \pm 2.709	69.509 \pm 1.709	72.958 \pm 0.419
+ FoSR	85.750 \pm 1.099	69.250 \pm 1.810	80.500 \pm 4.738	28.083 \pm 2.301	71.518 \pm 1.767	71.720 \pm 0.892
+ BORF	OOT	70.700 \pm 0.018	79.250 \pm 0.038	34.167 \pm 0.029	70.625 \pm 0.017	OOT
+ GTR	85.474 \pm 0.826	69.550 \pm 1.473	79.000 \pm 3.847	31.750 \pm 2.466	72.054 \pm 1.510	71.849 \pm 0.710
+ PANDA	90.325 \pm 0.867	68.350 \pm 2.346	83.250 \pm 3.262	42.167 \pm 2.286	72.321 \pm 1.786	73.320 \pm 0.814
+ EGP	77.875 \pm 1.563	68.250 \pm 1.121	81.500 \pm 4.696	40.667 \pm 3.095	70.848 \pm 1.568	72.330 \pm 0.954
+ CGP	78.225 \pm 1.268	71.650 \pm 1.532	85.250 \pm 3.200	50.083 \pm 2.242	73.080 \pm 1.396	73.350 \pm 0.788
+ SCGP	84.040 \pm 3.540	71.670 \pm 1.290	81.320 \pm 3.070	58.290 \pm 3.000	72.020 \pm 1.660	72.110 \pm 0.6800

Table 3: Training and Evaluation Time and Memory footprint on TU-Reddit Binary and TU-Collab.

Model	REDDIT-BINARY			COLLAB		
	Train Time	Eval. Time	Mem. (MB)	Train Time	Eval. Time	Mem. (MB)
GIN	0.1049 \pm 0.0237	0.0741 \pm 0.0032	922	0.2787 \pm 0.0345	0.2364 \pm 0.0094	1722
+ FA	OOM	OOM	OOM	0.4625 \pm 0.0507	0.4488 \pm 0.0404	4746
+ FoSR	0.1117 \pm 0.0268	0.0841 \pm 0.0164	906	0.3129 \pm 0.0386	0.2619 \pm 0.0257	3320
+ PANDA	0.7902 \pm 0.0597	0.7489 \pm 0.0439	1316	2.1152 \pm 0.0964	1.9347 \pm 0.0924	4406
+ EGP	0.1215 \pm 0.0257	0.0952 \pm 0.0128	976	0.3096 \pm 0.0372	0.2598 \pm 0.0164	1696
+ CGP	0.1326 \pm 0.0296	0.1147 \pm 0.0135	1128	0.3191 \pm 0.0321	0.2785 \pm 0.0160	2418
+ SCGP	0.2254 \pm 0.0064	0.0467 \pm 0.0017	287	0.5345 \pm 0.0065	0.1143 \pm 0.0023	266

Unlike prior approaches that require extensive preprocessing or suffer from out-of-memory (OOM) failures (e.g., BORF, FA), the SCGP method remains scalable and lightweight, integrating effortlessly into standard GNN workflows. By introducing structured coset-based expansions, SCGP enlarges the effective receptive field without over-parameterization, mitigating over-squashing while preserving spectral and topological integrity.

In addition, a fair comparison highlights that the observed performance gains can be directly attributed to the incorporation of structured embeddings introduced by SCGP. As shown in **Table 2**, under identical hyperparameter settings, SCGP demonstrates notable efficiency and effectiveness when compared to methods that rely on extensive preprocessing or the addition of virtual nodes.

In **Table 3**, SCGP exhibits a highly favorable computational efficiency profile. Although it introduces a slight increase in training time relative to baseline models such as GIN and CGP Wilson et al. [34], it substantially outperforms all competing methods in terms of evaluation speed and memory consumption due to the integration of structured embeddings during training. SCGP records the lowest memory usage on both REDDIT-BINARY and COLLAB, reinforcing its suitability for deployment in resource-constrained environments. Additionally, SCGP maintains consistently fast inference times, positioning it as a strong candidate for real-time and latency-sensitive applications.

To extend the evaluation to a real-world molecular prediction task, SCGP is assessed on the OGBG-MOLHIV dataset [18], a large-scale benchmark within the MoleculeNet suite [35] widely adopted for evaluating graph-based molecular property prediction models. The experimental protocol adheres to the open-source implementation and hyperparameter configuration specified by Hu et al. [18], with the number of layers fixed to 5, hidden dimensionality set to 300, a dropout rate of 0.5, and a batch size of 64.

Table 4: ROC-AUC (%) scores on the OGBG-MOLHIV Hu et al. [18] dataset. The results are averaged over 10 runs with standard deviation. SCGP achieves performance comparable to other structure-aware enhancements while maintaining generalization.

Model	OGB-M.
GCN	0.7566 ± 0.0104
+ Master Node	0.7531 ± 0.0128
+ FA	0.7628 ± 0.0191
+ EGP	0.7731 ± 0.0081
+ CGP	0.7794 ± 0.0122
+ SCGP	0.7823 ± 0.0119
GIN	0.7678 ± 0.0183
+ Master Node	0.7608 ± 0.0134
FA	0.7718 ± 0.0147
+ EGP	0.7537 ± 0.0076
+ CGP	0.7899 ± 0.0090
+ SCGP	0.7831 ± 0.0249

Comparative analyses include graph augmentation techniques such as Expander and Cayley Graphs [34]. **Table 4** reports ROC-AUC% metrics on the OGBG-MOLHIV dataset for various graph augmentation strategies applied to both GCN and GIN architectures. SCGP exhibits robust predictive performance while maintaining high structural fidelity and computational efficiency. Notably, SCGP—when integrated with either GCN or GIN—consistently surpasses models such as GCN + MasterNode and GCN + FA, outperforming augmentation schemes including CGP and EGP. SCGP achieves these gains without introducing auxiliary nodes or incurring the overhead associated with graph rewiring or truncation, thus offering a memory-efficient and theoretically grounded alternative.

5 Conclusion

This research presents **SCHREIER-COSET GRAPH PROPAGATION (SCGP)**, a novel and computationally efficient augmentation technique designed to address the over-squashing problem in Graph Neural Networks (GNNs). By leveraging group-theoretic embeddings derived from Schreier cosets of the special linear group $SL(2, (\mathbb{Z}_n))$, SCGP enhances long-range message propagation without modifying the graph topology or introducing auxiliary nodes. The resulting embeddings capture expansion-like properties in a compact form, improving both inference speed and memory efficiency. Unlike traditional rewiring strategies, SCGP encodes structural diversity within the node feature space, avoiding additional graph traversal costs. Comprehensive evaluation of node and graph classification benchmarks demonstrates that SCGP performs comparably to or exceeds state-of-the-art augmentation methods, particularly on hierarchical and modular graph structures. SCGP integrates seamlessly into standard GNN pipelines and offers a favorable trade-off between theoretical rigor and empirical effectiveness.

Future works. SCGP’s demonstrated efficacy across diverse graph typologies indicates considerable potential for its specialized application to planar or highly sparse structures, meriting further systematic investigation. Key research will enhance SCGP’s robustness and adaptability in these contexts, utilizing refined Schreier embedding deployment strategies for low-connectivity regimes and principled topology-aware augmentations to improve generalization. Moreover, SCGP’s performance sensitivity to group generator (S_n) and modulus n selection will be systematically investigated for optimal parameterization.

References

- [1] Sergi Abadal, Akshay Jain, Robert Guirado, Jorge López-Alonso, and Eduard Alarcón. Computing graph neural networks: A survey from algorithms to accelerators. *ACM Computing Surveys (CSUR)*, 54(9):1–38, 2021.
- [2] Noga Alon and Vitali D Milman. Eigenvalues, expanders and superconcentrators. In *25th Annual Symposium on Foundations of Computer Science, 1984.*, pages 320–322. IEEE, 1984.

- [3] Uri Alon and Eran Yahav. On the bottleneck of graph neural networks and its practical implications. *arXiv preprint arXiv:2006.05205*, 2020.
- [4] Adrián Arnaiz-Rodríguez, Ahmed Begga, Francisco Escolano, and Nuria Oliver. Diffwire: Inductive graph rewiring via the lov\’asz bound. *arXiv preprint arXiv:2206.07369*, 2022.
- [5] Pradeep Kr Banerjee, Kedar Karhadkar, Yu Guang Wang, Uri Alon, and Guido Montúfar. Oversquashing in gnns through the lens of information contraction and graph expansion. In *2022 58th Annual Allerton Conference on Communication, Control, and Computing (Allerton)*, pages 1–8. IEEE, 2022.
- [6] Mitchell Black, Zhengchao Wan, Amir Nayyeri, and Yusu Wang. Understanding oversquashing in gnns through the lens of effective resistance. In *International Conference on Machine Learning*, pages 2528–2547. PMLR, 2023.
- [7] Marc Brockschmidt. Gnn-film: Graph neural networks with feature-wise linear modulation. In *International Conference on Machine Learning*, pages 1144–1152. PMLR, 2020.
- [8] Olivier Chapelle, Bernhard Scholkopf, and Alexander Zien. Semi-supervised learning (chapelle, o. et al., eds.; 2006)[book reviews]. *IEEE Transactions on Neural Networks*, 20(3):542–542, 2009.
- [9] Andreea Deac, Marc Lackenby, and Petar Veličković. Expander graph propagation. In *Learning on Graphs Conference*, pages 38–1. PMLR, 2022.
- [10] Francesco Di Giovanni, Lorenzo Giusti, Federico Barbero, Giulia Luise, Pietro Lio, and Michael M Bronstein. On over-squashing in message passing neural networks: The impact of width, depth, and topology. In *International conference on machine learning*, pages 7865–7885. PMLR, 2023.
- [11] Vijay Prakash Dwivedi, Anh Tuan Luu, Thomas Laurent, Yoshua Bengio, and Xavier Bresson. Graph neural networks with learnable structural and positional representations. *arXiv preprint arXiv:2110.07875*, 2021.
- [12] Moshe Eliasof, Fabrizio Frasca, Beatrice Bevilacqua, Eran Treister, Gal Chechik, and Haggai Maron. Graph positional encoding via random feature propagation. In *International Conference on Machine Learning*, pages 9202–9223. PMLR, 2023.
- [13] Lukas Fesser and Melanie Weber. Mitigating over-smoothing and over-squashing using augmentations of forman-ricci curvature. In *Learning on Graphs Conference*, pages 19–1. PMLR, 2024.
- [14] Johannes Gasteiger, Stefan Weißenberger, and Stephan Günnemann. Diffusion improves graph learning. *Advances in neural information processing systems*, 32, 2019.
- [15] Justin Gilmer, Samuel S Schoenholz, Patrick F Riley, Oriol Vinyals, and George E Dahl. Neural message passing for quantum chemistry. In *International conference on machine learning*, pages 1263–1272. PMLR, 2017.
- [16] Will Hamilton, Zhitaoy Ying, and Jure Leskovec. Inductive representation learning on large graphs. *Advances in neural information processing systems*, 30, 2017.
- [17] Hengtao He, Xianghao Yu, Jun Zhang, Shenghui Song, and Khaled B Letaief. Message passing meets graph neural networks: A new paradigm for massive mimo systems. *IEEE Transactions on Wireless Communications*, 23(5):4709–4723, 2023.
- [18] Weihua Hu, Matthias Fey, Marinka Zitnik, Yuxiao Dong, Hongyu Ren, Bowen Liu, Michele Catasta, and Jure Leskovec. Open graph benchmark: Datasets for machine learning on graphs. *Advances in neural information processing systems*, 33:22118–22133, 2020.
- [19] Ningyuan Teresa Huang and Soledad Villar. A short tutorial on the weisfeiler-lehman test and its variants. In *ICASSP 2021-2021 IEEE International Conference on Acoustics, Speech and Signal Processing (ICASSP)*, pages 8533–8537. IEEE, 2021.
- [20] Kedar Karhadkar, Pradeep Kr Banerjee, and Guido Montúfar. Fcsr: First-order spectral rewiring for addressing oversquashing in gnns. *arXiv preprint arXiv:2210.11790*, 2022.
- [21] Thomas N Kipf and Max Welling. Semi-supervised classification with graph convolutional networks. *arXiv preprint arXiv:1609.02907*, 2016.

- [22] Devin Kreuzer, Dominique Beaini, Will Hamilton, Vincent Létourneau, and Prudencio Tossou. Rethinking graph transformers with spectral attention. *Advances in Neural Information Processing Systems*, 34:21618–21629, 2021.
- [23] Christopher Morris, Nils M Kriege, Franka Bause, Kristian Kersting, Petra Mutzel, and Marion Neumann. Tudataset: A collection of benchmark datasets for learning with graphs. *arXiv preprint arXiv:2007.08663*, 2020.
- [24] Khang Nguyen, Nong Minh Hieu, Vinh Duc Nguyen, Nhat Ho, Stanley Osher, and Tan Minh Nguyen. Revisiting over-smoothing and over-squashing using ollivier-ricci curvature. In *International Conference on Machine Learning*, pages 25956–25979. PMLR, 2023.
- [25] Ivan N Sanov. A property of a representation of a free group. In *Doklady Akad. Nauk SSSR (NS)*, volume 57, page 16, 1947.
- [26] Otto Schreier. Die untergruppen der freien gruppen. *Abhandlungen aus dem Mathematischen Seminar der Universität Hamburg*, 5(1):161–183, 1927. doi: 10.1007/BF02952517. URL <https://doi.org/10.1007/BF02952517>.
- [27] Prithviraj Sen, Galileo Namata, Mustafa Bilgic, Lise Getoor, Brian Galligher, and Tina Eliassi-Rad. Collective classification in network data. *AI magazine*, 29(3):93–93, 2008.
- [28] Oleksandr Shchur, Maximilian Mumme, Aleksandar Bojchevski, and Stephan Günnemann. Pitfalls of graph neural network evaluation. *arXiv preprint arXiv:1811.05868*, 2018.
- [29] Dai Shi, Andi Han, Lequan Lin, Yi Guo, and Junbin Gao. Exposition on over-squashing problem on gnns: Current methods, benchmarks and challenges. *arXiv preprint arXiv:2311.07073*, 2023.
- [30] Hamed Shirzad, Ameya Velingker, Balaji Venkatachalam, Danica J Sutherland, and Ali Kemal Sinop. Exphormer: Sparse transformers for graphs. In *International Conference on Machine Learning*, pages 31613–31632. PMLR, 2023.
- [31] Jake Topping, Francesco Di Giovanni, Benjamin Paul Chamberlain, Xiaowen Dong, and Michael M Bronstein. Understanding over-squashing and bottlenecks on graphs via curvature. *arXiv preprint arXiv:2111.14522*, 2021.
- [32] Petar Velickovic, Guillem Cucurull, Arantxa Casanova, Adriana Romero, Pietro Lio, Yoshua Bengio, et al. Graph attention networks. *stat*, 1050(20):10–48550, 2017.
- [33] Paul Werbos. Beyond regression: New tools for prediction and analysis in the behavioral sciences. *PhD thesis, Committee on Applied Mathematics, Harvard University, Cambridge, MA*, 1974.
- [34] JJ Wilson, Maya Bechler-Speicher, and Petar Veličković. Cayley graph propagation. *arXiv preprint arXiv:2410.03424*, 2024.
- [35] Zhenqin Wu, Bharath Ramsundar, Evan N Feinberg, Joseph Gomes, Caleb Geniesse, Aneesh S Pappu, Karl Leswing, and Vijay Pande. Moleculenet: a benchmark for molecular machine learning. *Chemical science*, 9(2):513–530, 2018.
- [36] Zonghan Wu, Shirui Pan, Fengwen Chen, Guodong Long, Chengqi Zhang, and Philip S Yu. A comprehensive survey on graph neural networks. *IEEE transactions on neural networks and learning systems*, 32(1):4–24, 2020.
- [37] Keyulu Xu, Weihua Hu, Jure Leskovec, and Stefanie Jegelka. How powerful are graph neural networks? *arXiv preprint arXiv:1810.00826*, 2018.
- [38] Chengxuan Ying, Tianle Cai, Shengjie Luo, Shuxin Zheng, Guolin Ke, Di He, Yanming Shen, and Tie-Yan Liu. Do transformers really perform badly for graph representation? *Advances in neural information processing systems*, 34:28877–28888, 2021.